Cancer Letters 454 (2019) 14–25

Contents lists available at ScienceDirect

Cancer Letters

journal homepage: www.elsevier.com/locate/canlet

Original Articles

Epigenetic regulation of UDP-Glucuronosyltransferase by microRNA-200a/-183: implications for responses to sorafenib treatment in patients with hepatocellular carcinoma

Yang Ge[a], Shuzhen Chen[b,c], Wei Mu[a], Qian Ba[a], Jingquan Li[a], Peizhan Chen[a], Xianming Wang[d,**], Hui Wang[a,*]

[a] Center for Single-Cell Omics, School of Public Health, Shanghai Jiao Tong University School of Medicine, Shanghai 200025, China
[b] Eastern Hepatobiliary Surgery Hospital, Second Military Medical University, 225 Changhai Road, Shanghai 200438, China
[c] National Center for Liver Cancer, Second Military Medical University, Shanghai, 200438, China
[d] Department of General Surgery, Qianfoshan Hospital Affiliated to Shandong University, Shandong, 250014, China

ARTICLE INFO

Keywords:
HCC
UGT1A9
miR-200a/-183
Sorafenib response

ABSTRACT

Patients receiving sorafenib treatment for hepatocellular carcinoma (HCC) experience different treatment efficacy. Personalized sorafenib treatment should be achieved through the identification of predictors of therapeutic response. In the current study, we found that high UGT1A9 expression indicated better prognosis for HCC patients treated with sorafenib after surgery. In silico analysis predicted microRNA-200a/-183 as potential regulators of the UGT1A gene family via binding to the shared UGT1A9 3′-UTR. A significant inverse correlation between microRNA-200a/-183 and UGT1A9 mRNA level was observed in a panel of HCC specimens. Direct binding was further demonstrated by luciferase reporter gene vector carrying wild-type or binding site truncated UGT1A9 3′-UTR. MicroRNA-200a/-183 downregulated UGT1A9 expression in a dose-dependent manner and significantly reduced sorafenib β-D-glucuronide formation in HCC cells. These data indicated that UGT1A9, under epigenetic regulation of microRNA-200a/-183, could predict patients who might benefit from adjuvant sorafenib treatment after surgery.

1. Introduction

Hepatocellular carcinoma (HCC) has become the most common primary hepatic malignancy, with a median survival between 6 and 20 months for patients, depending on the stage [1]. HCC now ranks fifth in the world among all malignancies and is the third leading cause of deaths attributed to cancer [2], with an annual incidence of 5–20/100,000, depending on geographic location [3]. The ratio of mortality and morbidity in liver cancer is as high as 0.96 [2]. Chronic liver disease secondary to hepatitis B virus (HBV) infection is the most common cause of HCC in China, while other major risk factors include non-alcoholic steatohepatitis, alcohol liver, aflatoxin, fatty liver, tyrosine metabolic disease and hepatitis C virus (HCV) infection in European and American countries [4].

Due to a lack of effective screening methods, the majority of patients with liver cancer are in advanced stages at the time of diagnosis [3]. Most patients with advanced disease have few options for treatment, including interventional therapy, radiation therapy, targeted therapy and other palliative treatments. In the past decade, molecular targeted drugs, such as sorafenib, have provided new options for treatment of advanced liver cancer [4]. However, five-year survival rate for advanced hepatic cancer remains less than 10% [5]. Sorafenib is the standard systemic treatment for patients with advanced HCC. However, its therapeutic value in patients with HCC after resection remains controversial. Importantly, individual patients have intrinsic differences in sensitivity to sorafenib treatment. Thus, how and when to use sorafenib in an individualized manner has become an urgent problem.

Sorafenib is primarily metabolized in the liver by oxidation of cytochrome P450 (CYP3A4) and glucuronidation of UGD glucuronosyltransferase 1A9 (UGT1A9) [6]. This drug has a half-life of approximately 25–48 h. Approximately 77% (50% of which is a drug prototype) of the active ingredient of sorafenib is found in feces, and approximately 19% is excreted in the urine (almost all drugs are either glucuronidated or intermediate metabolites without the original drug

* Corresponding author. Center for Single-Cell Omics, School of Public Health, Shanghai Jiao Tong University School of Medicine, Shanghai 200025, China.
** Corresponding author. Department of General Surgery, Qian Fo Shan Hospital affiliated to Shandong University, Shandong, 250014, China.
E-mail addresses: wangxianmingts@163.com (X. Wang), huiwang@shsmu.edu.cn (H. Wang).

https://doi.org/10.1016/j.canlet.2019.03.030
Received 9 December 2018; Received in revised form 19 March 2019; Accepted 20 March 2019

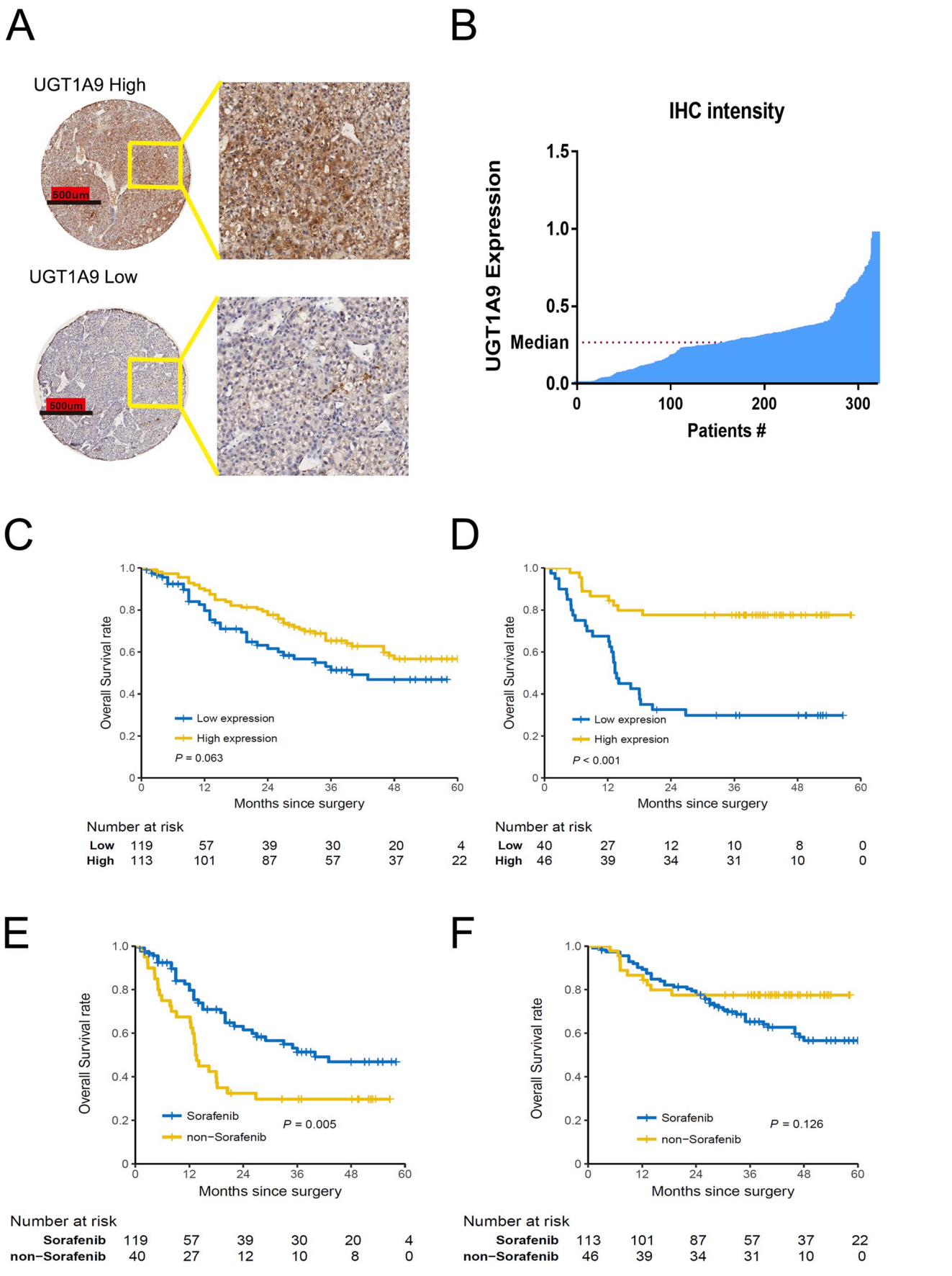

(caption on next page)

Fig. 1. UGT1A9 expression is associated with sorafenib response in patients with HCC. (**A**) Immunohistochemical staining of UGT1A9 in samples from patients. Representative picture was shown. **(B)** UGT1A9 expression was determined by immunohistochemistry staining in 318 cases of HCC tumor tissues by Image-scope software. (**C, D**) In patients treated with sorafenib, the prognosis of UGT1A9 high expression patients was better than that of patients with low expression. (E) Prognosis analysis of patients with or without sorafenib treatment in patients of high UGT1A9 expression. (F) Prognosis analysis of patients with or without sorafenib treatment in patients of low UGT1A9 expression.

component) [7]. Phase I (CYPs) and phase II (UGTs) metabolizing enzymes play vital roles in carcinogenesis and tumor response to anticancer therapy [8–10]. However, epigenetic regulation of UGT1A9 and its clinical implications have not been systematically examined in patients with HCC. A recent report showed that epigenetic regulation of noncoding RNA was implicated in drug metabolism and efficacy; however, the exact mechanism of action remains to be clarified.

Since changes in sorafenib metabolism by altering CYP3A4 or UTG1A9 activity may affect its clinical efficacy and sorafenib-induced toxicity, our study aimed to explore the epigenetic regulation of UGT1A9 by miRNA and to evaluate whether expression of UGT1A9 is associated with response to sorafenib treatment in HCC patients. These results provide valuable information for sorafenib treatment in a clinical setting.

2. Materials and methods

2.1. Patients and samples

Three hundred and eighteen samples were randomly retrieved from HCC patients who underwent curative resection at Eastern Hepatobiliary Surgery Hospital, Shanghai, China, from June 2007 to July 2010. A second cohort of sorafenib treatment patients (N = 52) were also obtained from Eastern Hepatobiliary Surgery Hospital, Shanghai, China, from June 2007 to July 2010 with median follow-up of 48 months. Patients treated with oral sorafenib received a dose of 200–800 mg/d within 30 d after surgery. In the event of drug-related adverse effects, the dose was reduced to 200 mg twice daily (Supplemental Table 1). All patients were followed until March 2014, with a median observation time of 48 months. Overall survival (OS) was defined as the interval between the dates of surgery and death. If recurrence was not diagnosed, patient data were censored on the date of death or the last follow-up. Primary HCC samples and adjacent normal liver tissues were used in the construction of a tissue microarray. Immunostaining of UGT1A9 was performed on tissue microarray slides. Assessment of staining was based on the percentage of positively stained cells and staining intensity using ImageScope software (Media Cybernetics, Inc.). All samples were obtained after informed consent according to an established protocol approved by the Ethic Committee of the Eastern Hepatobiliary Surgery Hospital.

2.2. Cells, reagents, and plasmids

HCC cell lines and 293T were obtained from Shanghai Cell Bank (Shanghai, China). Cell lines were routinely cultured in DMEM medium (Invitrogen) supplemented with 10% fetal bovine serum (FBS, Gibco) within a humidified incubator containing 5% CO_2 at 37 °C. PMIR-report and PMIR-control dual luciferase reporter plasmids were provided by Prof. Zhou from the Academy of Military Medical Science, Beijing. The wild-type 3′-UTR of the UGT1A9 gene was cloned into the reporter plasmid, and the truncated mutation of the miRNA target site was induced by overlapping extension PCR. All miRNA mimics and their controls were purchased from RiboBio Co., Guangzhou, China. For studies in 12-well plates, miRNA mimics were transfected into corresponding cells (100 nM/well) for 12 h, and the medium was then changed. Experiments for detection were performed 24 or 48 h after transfection.

2.3. Luciferase activity assay

Cell lysates (10 μl) were assayed in the presence of 100 μl luciferase assay buffer (25 mM glycyl-glycine, 15 mM $MgSO_4$, 5 mM ATP, and 6.25 μM D-luciferin). Luciferase activity was measured with a Synergy 2 Multi-detection Microplate Reader (BioTek Instruments, Inc.).

2.4. Immunohistochemistry staining

Immunohistochemistry of paraffin-embedded xenograft tumors or tissue microarray slides was performed using primary antibodies. Briefly, slides were probed with primary antibodies specific for UGT1A9 (ABclonal Technology) and anti-rabbit horseradish peroxidase-conjugated secondary antibodies (Santa Cruz Biotechnology, Santa Cruz, CA). Diaminobenzidine colorimetric reagent solution from Dako (Carpinteria, CA) was used to visualize the signal and was followed by hematoxylin counterstaining (Sigma Chemical Co).

2.5. RNA extraction and real-time polymerase chain reaction (RT-PCR)

Total RNA was extracted from cultured cell lines or tumor tissues using Trizol reagent (Invitrogen) following the manufacturer's instructions. Reverse transcription PCR was performed using Superscript III RT (Invitrogen) in the presence of random primers. The generated cDNA was used to amplify indicated genes using specific primers (UGT1A9 Forward Primer: CCCCCTTCCTCTATGTGTGTG; Reverse Primer: TCAT ACTCCGTAACAGGTGTTTG) in SYBR Green PCR Master Mix (Takara) with ABI PRISM 7300HT Sequence Detection System. miRNA level was detected by using the Bulge-Loop™ miRNA qPCR Primer Set (RiboBio Co. Guangzhou, China). Each measurement was performed in triplicate, and results were normalized to expression of the 18S reference gene.

2.6. LC-MS analysis

Tissue samples were extracted from tumors and livers weighing about 50 mg with methanol and detected by Mass Spectrometry. Cell samples was extracted with ice methanol after sorafenib treatment. The Agilent 1100 Series high-performance liquid chromatograph, including the binary pump, online degasser, autosampler, and column oven, was used. Mass spectrometry uses the Agilent 1946 single quadrupole. Chromatographic separations were performed using a Waters X-select HSS T3 column (3.5 μm, 3.0 × 100 mm; Waters, Milford, MA, USA) at room temperature. The mobile phase was water (containing 0.1% formic acid) and acetonitrile (30:70, v:v) at a flow rate of 0.4 ml/min. The mass spectrometric scan was a selective ion monitoring (SIM) scan. Sorafenib metabolites and testosterone were detected at *m/z* 641.2 and *m/z* 289.4, respectively. The other mass spectrometry parameters were as follows: dry gas flow rate, 11.0 L/min; atomizing gas pressure, 45 psi; dryer temperature, 350 °C; and capillary voltage, 3500 V.

2.7. Animals and in vivo experiments

Male nude mice (6–8 weeks old) were obtained from the Chinese Science Academy, Shanghai, China. All the mice were maintained in individual microisolator cages (less than 4 mice per cage) under pathogen-free conditions. They have received human care according to the criteria outlined in the *Guide for the Care and Use of Laboratory Animals*, prepared by the National Academy of Sciences and published by the National Institutes of Health.

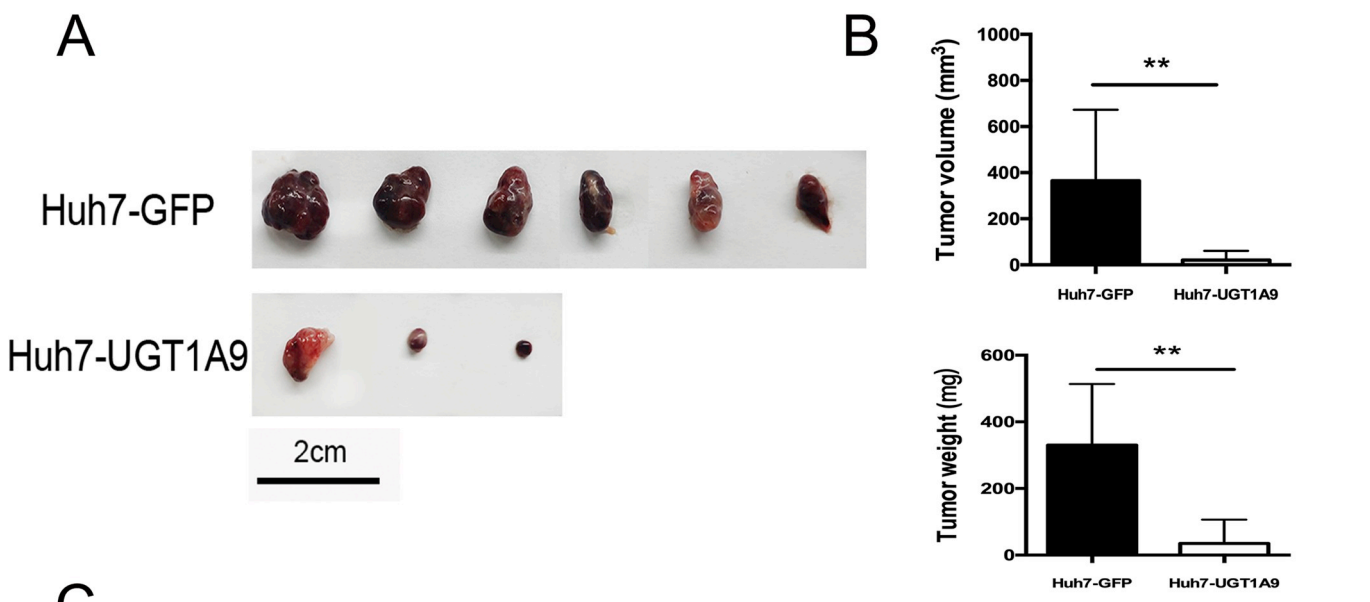

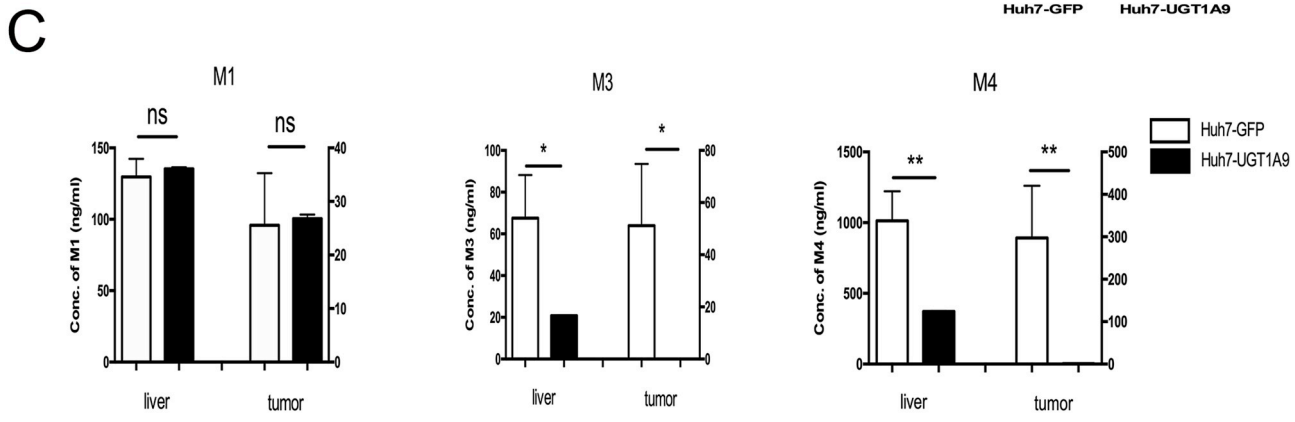

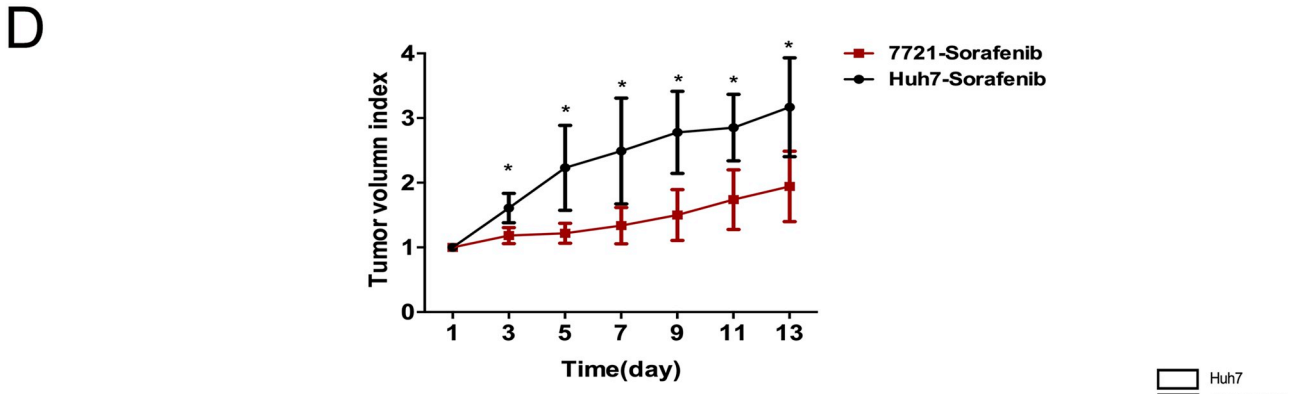

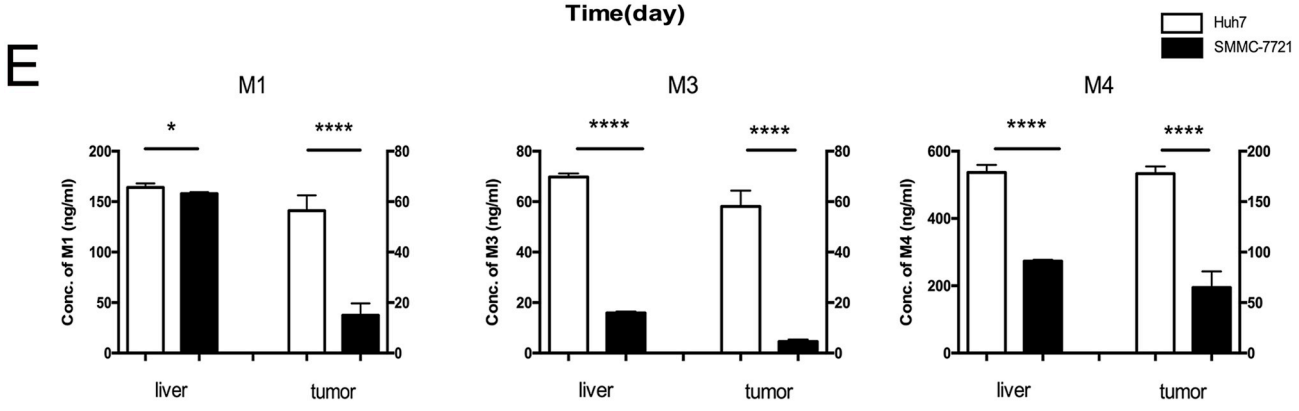

(caption on next page)

Fig. 2. UGT1A9 expression is associated with sorafenib response in mice xenograft models. (**A**) Dissected tumors from nude mice after implantation of Huh7-GFP (n = 8) or Huh7-UGT1A9 (n = 9). **(B)** Tumor volume and tumor weight of mice xenografts were calculated. (**C**) Sorafenib metabolites M1, M3 and M4 levels were detected by mass spectrometry in Huh7-GFP and Huh7-UGT1A9 derived xenografts and mice livers. (**D**) Tumor volume index of Huh7 (n = 4) and SMMC-7721 (n = 5) after sorafenib treatment were analyzed. (**E**) Sorafenib metabolites M1, M3 and M4 levels were detected by mass spectrometry in Huh7 and SMMC-7721 derived tumors and mice livers. Bars are mean ± SD of triplicate experiments. *$p < 0.05$, ****$p < 0.0001$.

To generate murine xenograft models, 2×10^6 HCC cells in 100 μl normal saline were injected subcutaneously to the right of the dorsal midline in nude mice. Once the tumors reached 100–200 mm^3, mice were randomly allocated into control groups or sorafenib treatment group. Mice were treated with sorafenib (60 mg/kg, once a day, S1040, Selleck) or DMSO for two weeks. Tumors were measured every other day and tumor volumes were calculated using the formula length × $width^2/2$. At Day 15 of sorafenib treatment, mice were sacrificed. Liver sample and xenograft sample were collected for later use.

2.8. Statistical analysis

Differences among variables were assessed using a two-tailed student's *t*-test. Data are presented as the mean ± standard error unless otherwise indicated. A *p*-value < 0.05 was considered statistically significant. Cumulative survival time was calculated using the Kaplan-Meier method and analyzed by the log-rank test. Univariate and multivariate analyses were based on the Cox proportional hazards regression model. Statistical analyses were performed using SPSS 16.0 software (SPSS, Chicago, IL, USA).

3. Results

3.1. UGT1A9 expression is associated with sorafenib response in patients with HCC

To explore the roles of UGT1A9 in HCC development and progression, we used immunohistochemical staining to evaluate expression of UGT1A9 in patient samples. Three hundred and eighteen samples of HCC tumor tissue were immunostained on tissue microarray. Most neoplastic cells showed cytoplasmic staining for UGT1A9. Representative pictures are shown in Fig. 1A. UGT1A9 expression over median intensity showed moderate to strong positive staining (Fig. 1B). These data indicated that expression of UGT1A9 displayed high heterogeneity in tumor tissues from HCC patients.

Established data show that phase I (CYPs) and II (UGTs) metabolizing enzymes play vital roles in the response to anticancer therapy. As UGT1A9 is a major phase II metabolizing enzyme of sorafenib, we analyzed the clinical relevance of UGT1A9 expression in patients with hepatocellular carcinoma treated with sorafenib after surgery. The intensity of immunohistochemical staining was evaluated using ImageScope scoring software. Median values of included patients were used as a group reference for high and low expression of UGT1A9. The distribution of basic clinicopathological features of tissue microarrays of patients with or without sorafenib treatment after surgery is shown in Supplemental Table 1.

Although no significant benefit was observed in patients treated with sorafenib after surgery (Supplemental Fig. 1, Supplemental Tables 1–4), we found that the prognosis of sorafenib-treated patients with high UGT1A9 expression was significantly better than for those in the control group (Fig. 1C&D). There was no difference in prognosis for patients with low expression of UGT1A9, regardless of whether they received sorafenib treatment (Fig. 1F). Patients with high expression of UGT1A9 exhibited a better response to sorafenib than patients with low expression of UGT1A9 (Fig. 1E&F, Supplemental Tables 1 and 2).

3.2. UGT1A9 expression is associated with sorafenib response in mice xenograft models

To explore the role of UGT1A9 expression on sorafenib response, first we examined the level of UGT1A9 in multiple HCC cell lines and 293T. In the cell lines detected, MHCC-97H and SMMC-7721 showed high level of UGT1A9, while in other HCC cell lines (Huh7, HCC-LM3 etc.), the level of UGT1A9 was rather low (Supplementary Fig. 1B). Based on this finding, UGT1A9 stable overexpressing cell line was established in Huh7. We inoculated Huh7-UGT1A9 cell line and its counterpart subcutaneously in nude mice. Four weeks after HCC inoculation, more and larger tumors were generated from mice implanted with Huh7-GFP as indicated by Fig. 2A&B. These mice were then randomly divided into two groups and treated with DMSO or sorafenib respectively for 2 days before livers and xenografts were collected for sorafenib metabolites analysis. To achieve a comprehensive understanding of alteration of sorafenib metabolism induced by miR-200a-3p/-183–5p, the sorafenib metabolites from CYP system (M1, M3 and M4), were detected. The data suggested M3 and M4 were significantly reduced both in liver and xenografts when UGT1A9 was overexpressed (Fig. 2C), indicating a decreased metabolism of sorafenib by CYP system. Since cancer stem cell plays a role on drug resistance, we have examined the expression of CD90, CD133, Epcam and Lgr5 in Huh7 cell lines. As expected, the expression of cancer stem cell markers was also decreased in Huh7-UGT1A9 than control cells (Supplementary Fig. 1C). We also observed that sorafenib treatment could inhibit the growth of SMMC-7721 (UGT1A9 high expressing HCC cells) more than Huh7 (UGT1A9 low expressing HCC cells) in mice xenograft models as indicated by increased tumor volume index of SMMC-7721 (Fig. 2D). Sorafenib metabolites analysis also showed an inhibition of CYP system products (Fig. 2E). These data demonstrated that enhanced expression of UTG1A9 is associated with better efficacy of sorafenib treatment.

3.3. miRNAs that might potentially bind to UGT1A9 mRNA were screened in vitro

Although polymorphisms of UGT1A family members have been reported, the discrepancy of UGT1A9 protein expression in patients with HCC has not been explained. To investigate the mechanism of UGT1A9 expression regulation, in silico analysis was used to explore miRNA binding to UGT1A mRNA. mRNA corresponding to the UGT1A 3′-UTR was analyzed using the miRanda (v3.0), miRDB and Target Scan algorithms to identify miRNAs that could target UGT1A9 mRNAs. The different subtypes of UGT1A family members have different first exons but share exons 2–5 and 3′-UTR (Fig. 3A). Three databases were used to predict complementarity and high fidelity. miRNAs were considered as upstream candidates if it was predicted by two software programs. Ultimately, 47 candidate miRNAs were identified (Fig. 3B). To verify the effects of candidate miRNAs on UGT1A9 expression, we detected the expression of UGT1A9 after transfection of miRNA mimics in SMMC-7721 cells for 48 h. Results showed that 12 miRNAs reduced UGT1A9 expression by 50% (MiR-548a-5p, MiR-548e-5p, MiR-4769–3p, MiR-4795–3p, MiR-491–3p, MiR-148a-3p, MiR-3646, MiR-4496, MiR-200a-3p, MiR-183–5p, MiR-548h-5, MiR-3908) (Fig. 3C). These miRNAs were included in subsequent studies.

Transfection with miRNA mimics may result in off-target effects, indirectly causing downregulation of UGT1A9 expression. To rule out this problem and demonstrate miRNA binding on the target gene 3′-UTR, which results in downregulation of target gene expression, we

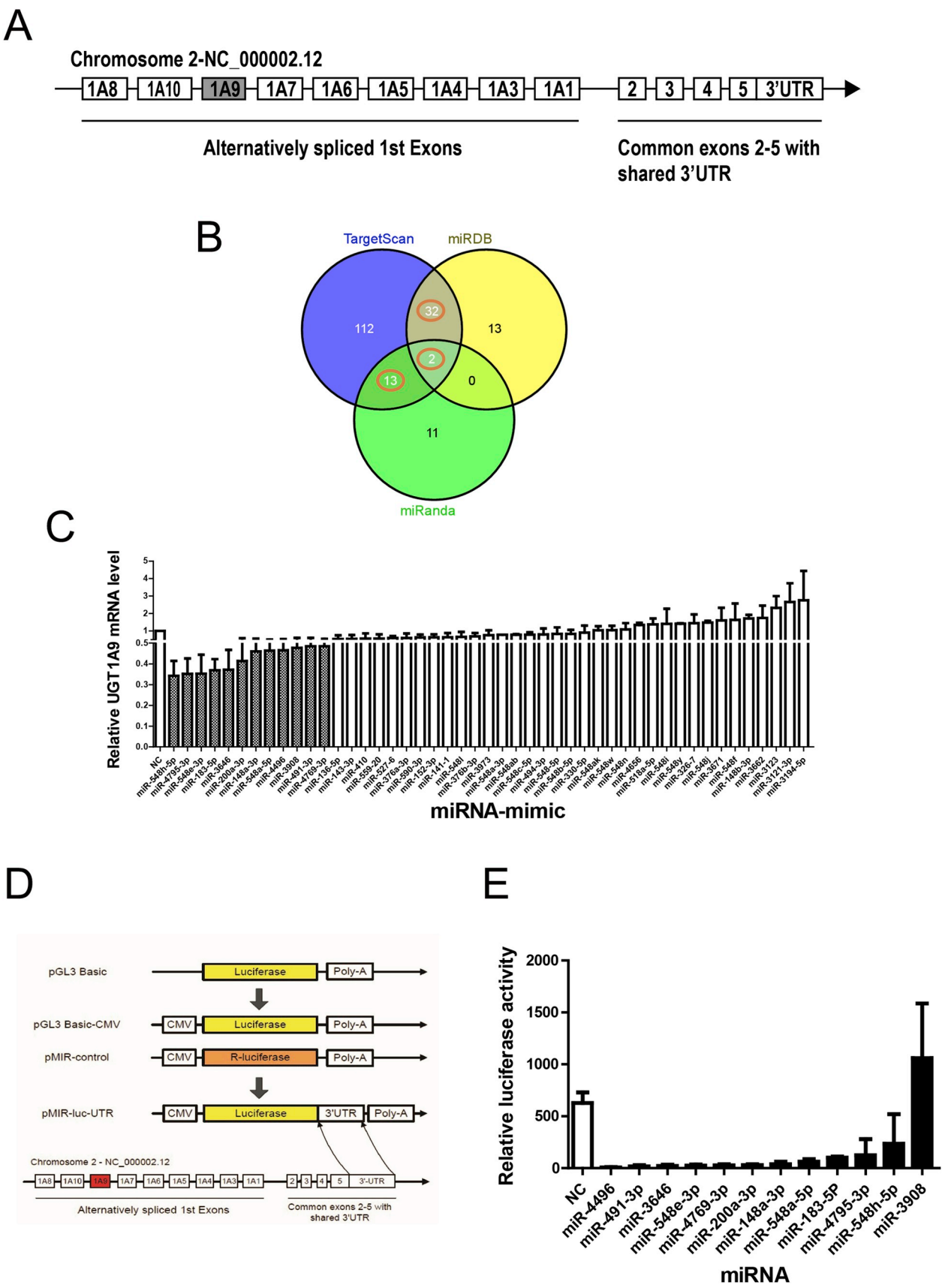

Fig. 3. MiRNA potentially binding to UGT1A9 mRNA was screened *in vitro*. (**A**) Gene loci structure of UGT1A. The nine alternative UGT1A first exons code for unique enzymes. **(B)** The three-way Venn diagram were used to identify miRNA potentially binding to 3′-UTR of UGT1A9. **(C)** UGT1A9 mRNA expression was detected in SMMC-7721 48 h after mimics of candidate miRNAs transfection. **(D)** Construction of a 3′-UTR reporter plasmid for UGT1A9 Expression. **(E)** Plasmid and candidate miRNA were co-transfected into 293T cells. Luciferase activity was detected 48 h later. Bars are presented as mean ± SD of triplicate wells per treatment condition.

Table 1
miRNA expression and correlation with UGT1A9 in HCC patients.

Expression of miRNAs in HCC		
No expression	Correlation with UGT1A9 expression	
	Negative correlation	No correlation
miR-548a-5p miR-548e-5p miR-4769–3p	miR-200a-3p miR-183–5p	miR-4795–3p miR-491–3p miR-148a-3p miR-3646

constructed a 3′-UTR double fluorescent reporter gene plasmid expressing UGT1A9 (Fig. 3D). Reporter plasmids and candidate miRNAs were cotransfected into 293T cells. Candidate miRNAs were screened using luciferase assay. Results showed that 11 of 12 miRNAs (excluding miR-3908) might act on the UGT1A9 3′-UTR (Fig. 3E).

3.4. A negative correlation between miR-200a/-183 and UGT1A9 was identified in clinical samples

Although *in silico* analysis predicted miRNAs that might act on the 3′-UTR of UGT1A9, whether the molecular mechanism existed *in vivo* required further investigation. Therefore, we collected samples of tumors and adjacent normal tissues from 48 patients with HCC. To determine miRNAs that regulate UGT1A9 *in vivo*, the correlation between UGT1A9 expression and candidate miRNAs in liver cancer and adjacent tissues was analyzed. We found that miR-548a-5p, miR-548e-5p, and miR-4769–3p were not expressed in liver cancer or adjacent tissues. miR-4795–3p, miR-491–3p, miR-148a-3p, miR-3646, miR-4496, and miR-548h-5p were expressed in hepatocellular carcinoma and adjacent tissues, but only one of these correlated with UGT1A9 expression (Table 1, Supplemental Fig. 2). In contrast, miR-183–5p and miR-200a-3p were negatively correlated with UGT1A9 expression in tissues samples ($P < 0.05$) (Fig. 4A–D). UGT1A9 is also widely expressed in organs such as kidney, small intestine, colon, and stomach [11]. To further confirm the regulation of miR-183–5p and miR-200a-3p on UGT1A9, we collected liver, kidney, duodenum, colon, stomach, spleen and pancreas biopsy tissues from patients. Consistent with our hypothesis, miR-183–5p, miR-200a-3p, and UGT1A9 expression revealed a pattern of negative correlation in most of these organs (Fig. 4E–F).

3.5. Site mutation verified binding of miR-200a/-183 to the UGT1A 3′-UTR

To further confirm miR-200a-3p and miR-183–5p regulation of UGT1A9, overlap PCR was used to construct binding site truncated mutation in dual fluorescence reporter plasmids carrying the 3′-UTR of UGT1A9 (Fig. 5A). Dual fluorescent reporter plasmids, miR-200a-3pand miR-183–5p, were cotransformed into 293T cells followed by detection using dual fluorescent reporter assays. There was no significant difference in luciferase enzyme activity in the mutated group compared to the control group. In contrast, the wild-type 3′-UTR of UGT1A9 resulted in significant downregulation of the reporter gene (Fig. 5B&C). To further confirm the effect of miR-200a-3p and miR-183–5p on the regulation of UGT1A9 expression, we have constructed miR-200a-3p stable expression cell line in SMMC-7721 and miR-183–5p stable expression cell line in Huh7. We have observed a decrease of UGT1A9 in miR-200a-3p or miR-183–5p overexpressing cell lines (Fig. 5D&E). These data demonstrated that miR-200a-3p and miR-183–5p directly act on the 3′-UTR of the target gene UGT1A9.

3.6. Effects of miR-200a/-183 on UGT1A expression and glucuronidation activity

miR-200a-3p and miR-183–5p transfection in SMMC-7721 cells induced UGT1A9 downregulation in a dose-dependent manner (Fig. 6A–B). As a marker of UGT1A9 enzyme activity, sorafenib β-D-glucuronide formation was monitored in homogenates from SMMC-7721 cells transiently transfected with miR-200a-3p and miR-183–5p mimic versus scrambled miRNA-transfected controls. In SMMC-7721 cell homogenates, sorafenib β-D-glucuronide formation was significantly reduced by over 75% ($P < 0.01$) in response to transfection of miR-200a-3p or miR-183–5p compared with scrambled miRNA-transfected controls (Fig. 6C).

To test the effect of miR-200a-3p and miR-183–5p on sorafenib response. We detected sorafenib metabolites in miR-200a-3p/-183–5p overexpressing cell lines. As data indicated by Fig. 6D&E, CYP system metabolites (M1, M3, M4) were accumulated significantly at LM3 miR-200a-3p/-183–5p overexpressing cell lines. M1 and M3 were also increased in 7721 miR-200a-3p cell line. These data together indicated an altered pharmacokinetic distribution of sorafenib metabolites regulated by miR-200a-3p/-183–5p.

We found that high UGT1A9 expression predicted a good prognosis in patients treated with sorafenib. Sorafenib is primarily metabolized by the oxidation of cytochrome P450 (CYP3A4) and the glucuronidation of glucuronosyltransferase 1A9. Glucuronidation of glucuronosyltransferase 1A9 increases the water solubility of lipid-soluble sorafenib and transports it out of the cell via MRCP, MRP-2 and P-gp transporters [12]. Meanwhile, we found that expression of transporters MRCP, MRP-2 and P-gp were significantly decreased in cancer tissues (data not shown). We speculated that sorafenib metabolites might accumulate in tumor cells, leading to cumulative dose increase and this might be the reason why prognosis of patients with high expression of UGT1A9 is better than that of patients with low UGT1A9 expression. The hypothetical model of this effect is illustrated in Fig. 6F.

4. Discussion

Sorafenib is a low-solubility, high-permeability drug that absorbs particularly rapidly and peaks in the blood 3 h after oral administration. Sorafenib is primarily metabolized in the liver by oxidation of cytochrome P450 (CYP3A4) and glucuronidation of glucuronosyltransferase 1A9 [13]. In humans, most (77%) of the sorafenib dose is either absorbed or eliminated through the hepatobiliary route (50% unchanged), while 19% of the dose (mostly glucuronides) is excreted in the urine [14]. Both routes of elimination require glucuronidation catalyzed by UGT1A9 [6].

UGT1A family members exhibit extensive interindividual variability in expression that results in variability in patient response and toxicity [15]. HNF4α was identified as a major factor for the control of UGT1A9 hepatic expression by corresponding promoter sequences [16]. Although polymorphisms in UGT genes and altered transcriptional regulation can contribute to altered expression and/or activity of UGT1A enzymes [17–20], these mechanisms do not explain the mismatch of UGT1A mRNA and protein levels [21–23]. Furthermore, there is a high degree of disparity in UGT mRNA and protein expression within different tissues and between different individuals [21,24]. Such observations suggest an epigenetic mechanism of posttranscriptional regulation may be involved in UGT protein expression.

MicroRNAs are known to play key roles in cancer and function as regulators of gene expression and cellular metabolism [25,26]. However, the roles of miRNAs in xenobiotic metabolism and in toxicology have only recently been explored. Recent research has highlighted the link between miRNA-related pharmacogenomics and drug reactions [27]. It was reported that microRNA 491–3p regulates UGT1A1 expression and activity [28]. We confirmed the theoretical binding of microRNA 491–3p and the 3′-UTR of UGT1A9, but no correlation was

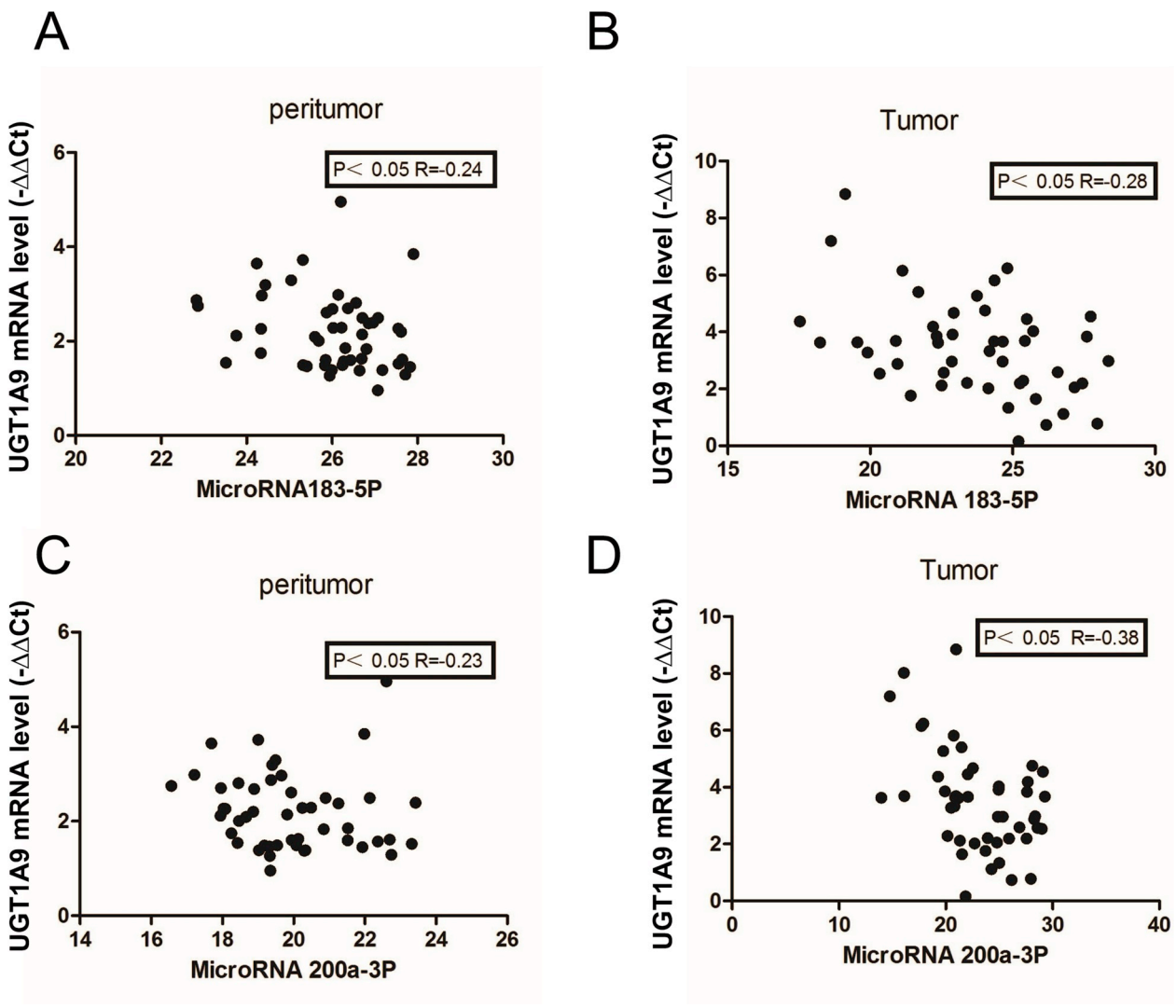

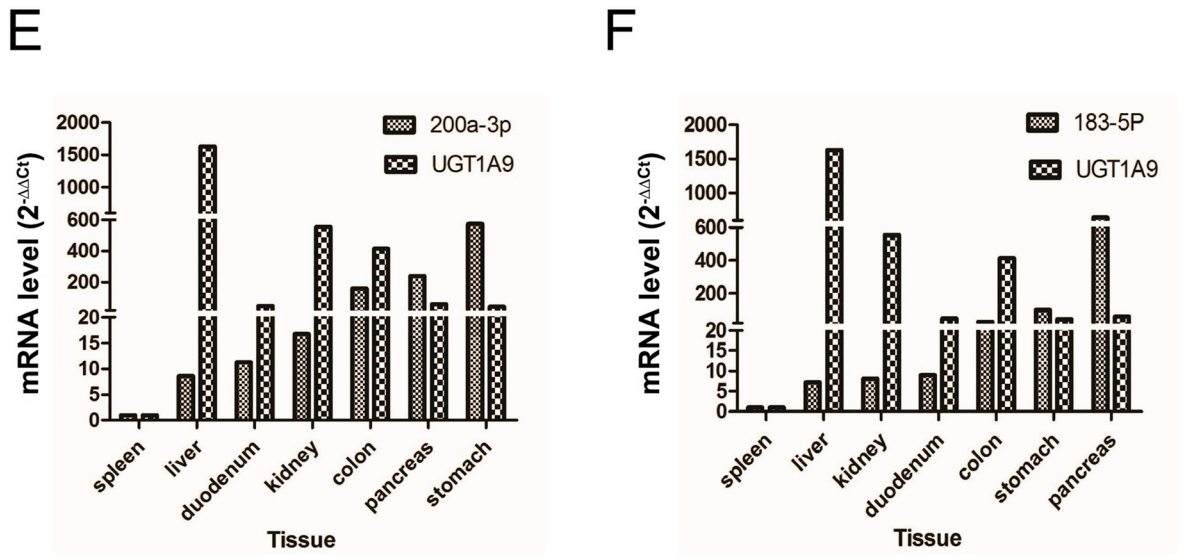

(caption on next page)

Fig. 4. Negative correlation of miR-200a/-183 and UGT1A9 was found in clinical samples. (**A, B**) Real-time PCR detection of miR-183–5p and UGT1A9 expression in hepatocellular carcinoma and adjacent tissues. SPSS statistical software analysis revealed negative correlation. (**C, D**) Real-time PCR detection of miR-200a-3p and UGT1A9 expression in hepatocellular carcinoma and adjacent tissues.SPSS statistical software analysis revealed negative correlation. (**E, F**) The expression of UGT1A9 and miR-200a/-183 were determined by RT-PCR in different biopsy tissues of patients, showing a negative correlation of miR-183–5p and miR-200a-3p with UGT1A9.

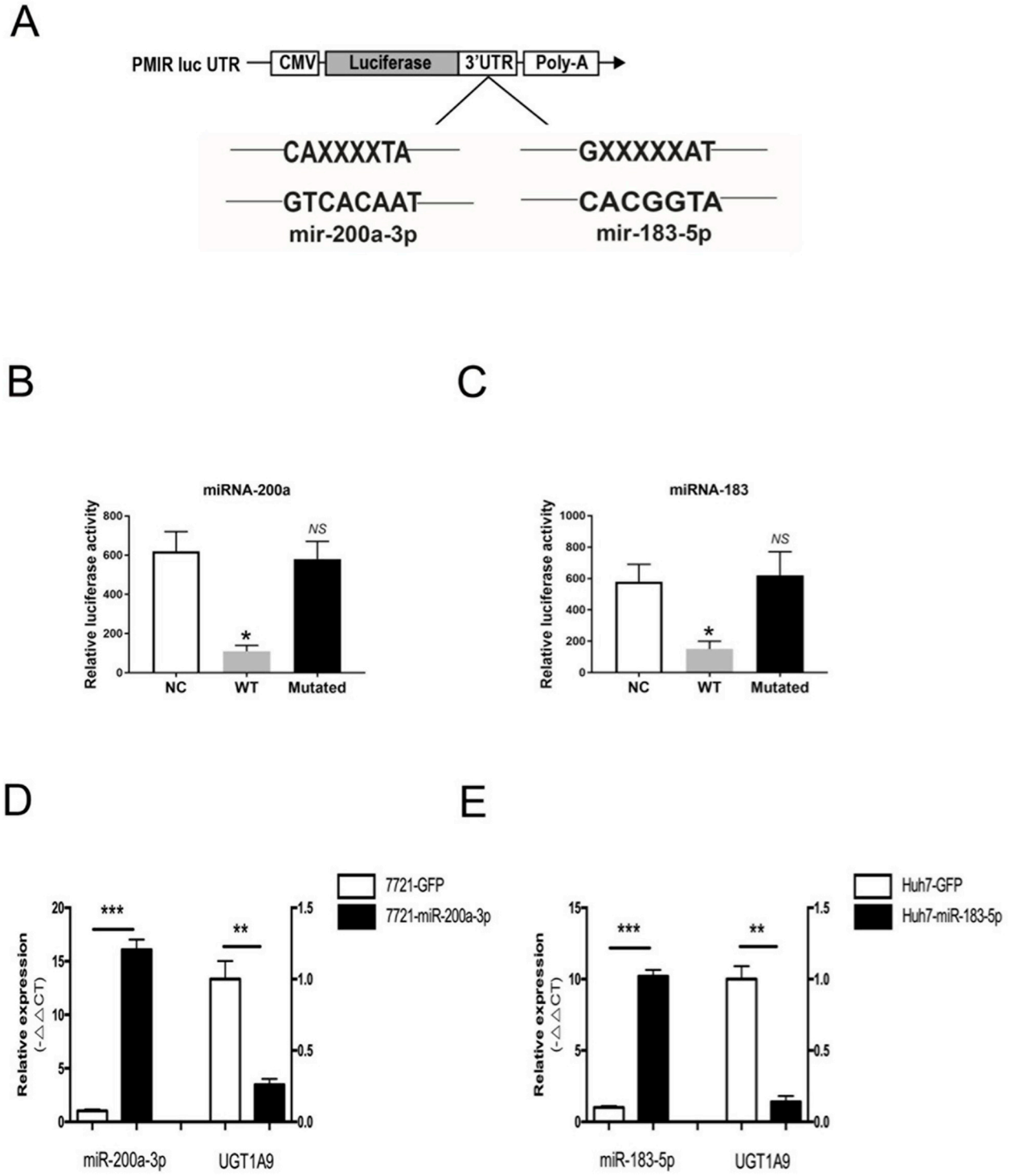

Fig. 5. Site mutation verified binding of miR-200a/-183 on UGT1A 3′-UTR. (**A**) Schematic diagram of truncated mutation of miR-200a/-183 binding site in UGT1A9 3′-UTR. **(B, C)** UGT1A9 3′-UTR reporter gene plasmid, miR-200a-3p and miR-183–5p mimics was co-transfected in 293T cells, respectively. Luciferase enzyme activity was detected 48 h later. (**D**) Real-time PCR detection of miR-200a-3p and UGT1A9 expression in 7721-GFP and 7721- miR-200a-3p. (**E**) Real-time PCR detection of miR-183–5p and UGT1A9 expression in Huh7-GFP and Huh7-miR-183–5p. Bars are mean ± SD of triplicate wells per treatment condition. *$p < 0.05$; ** $p < 0.01$; ***$p < 0.001$.

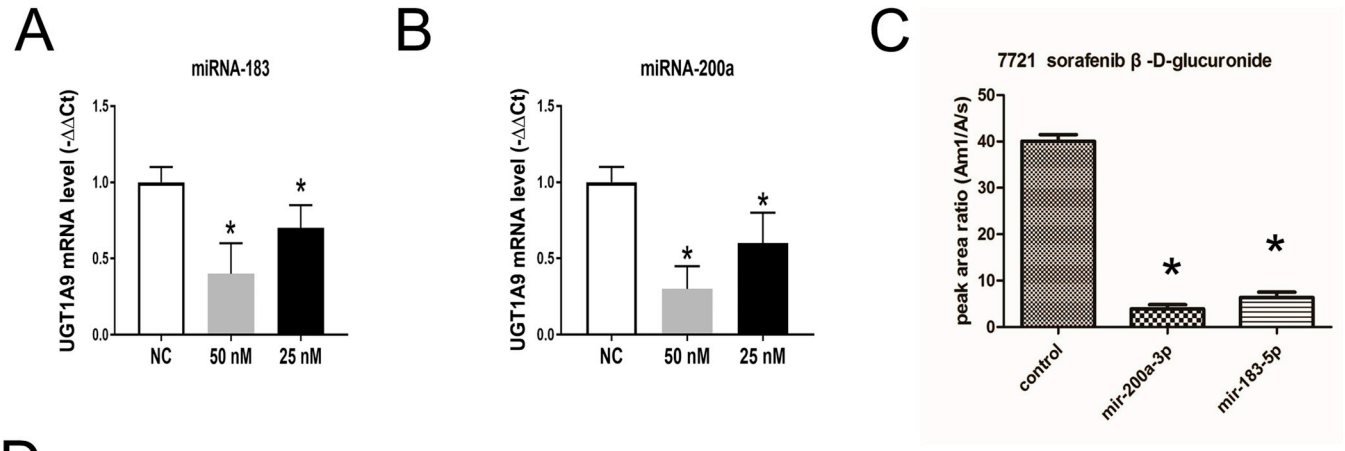

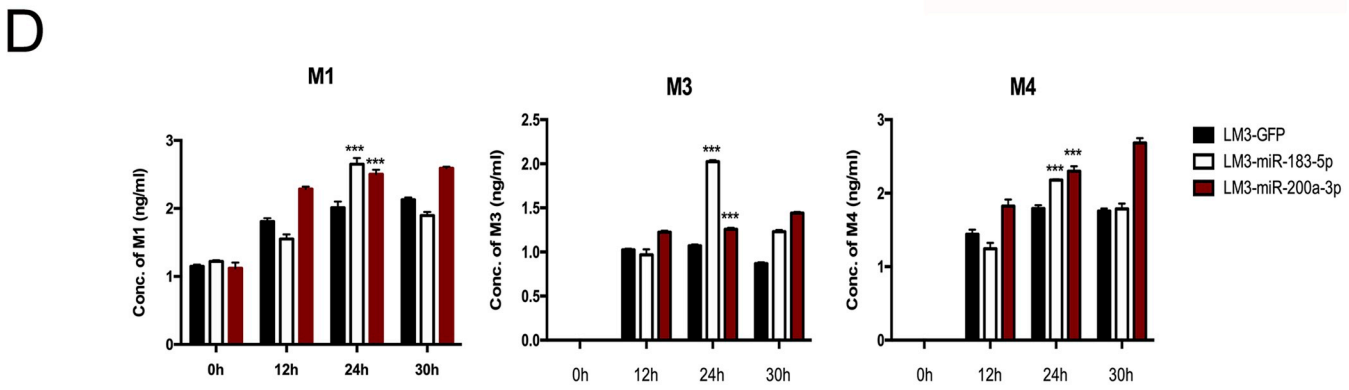

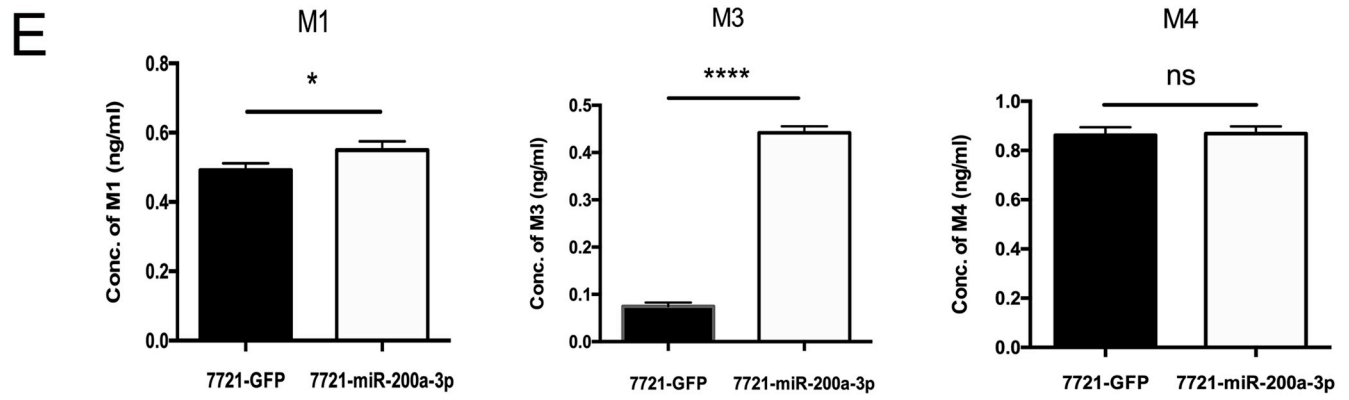

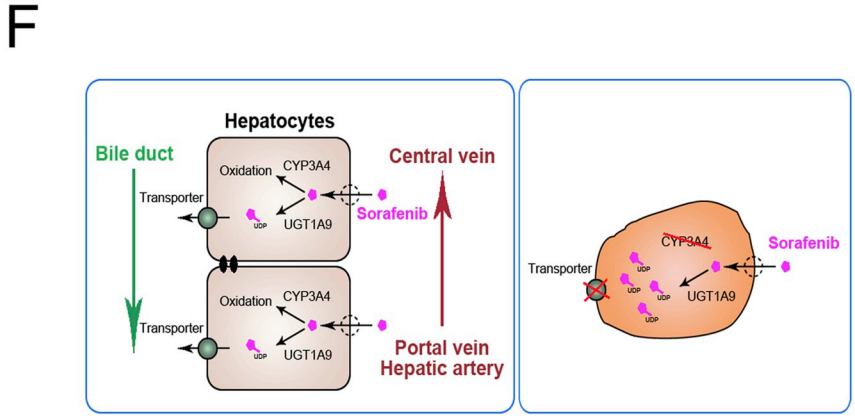

(caption on next page)

Fig. 6. Effects of miR-200a/-183 on UGT1A Expression and Glucuronidation Activity. (**A, B**) miR-200a-3p and miR-183–5p mimics was transfected in SMMC-7721 cells.The expression of UGT1A9 was determined by RT-PCR. **(C)** Sorafenib metabolites was detected by LC-MS analysis in miR-200a-3p and miR-183–5p mimics transfected SMMC-7721 cells. **(D)** Sorafenib metabolites M1, M3 and M4 levels were detected by mass spectrometry in LM3-GFP, LM3-miR-183–5p and LM3-miR-200a-3p cell lines treated with sorafenib at 0h, 12h, 24h and 30h. **(E)** Sorafenib metabolites M1, M3 and M4 levels were detected by mass spectrometry in 7721-GFP and 7721- miR-200a-3p treated with sorafenib at 24h. Bars are mean ± SD of triplicate results. *$p < 0.05$;** $p < 0.01$; ***$p < 0.001$; ****$p < 0.0001$. **(F)** A hypothetical model of UGT1A9 on sorafenib response in HCC cells.

observed between microRNA 491–3p and UGT1A9 in clinical samples of HCC (Table 1). In our study, post-transcriptional regulation of miR-183–5p and miR-200a-3p on UGT1A9 expression was demonstrated by fluorescent reporter assays and a 3′-UTR truncated mutant double fluorescent reporter gene plasmid.

Eight metabolites of sorafenib have been identified (M1-8) [6,29]. Among them, sorafenib N-oxide (M2) is produced through oxidation of sorafenib by CYP3A4 [30]. M2 and N-methylhydroxylation (M3) also get further metabolized to N-hydroxymethyl-sorafenib-N-oxide (M1) [31] and followed by clearance of drugs. However, the metabolite M7 (glucuronide of sorafenib) is produced through glucuronidation of the parent compound by UGT1A9, which is responsible for secondary maxima of the plasma concentration by reabsorption of sorafenib through enterohepatic recycling [32].

It is challenging to simply simulate metabolic processes *in vitro* using a cell culture system. M7 production was significantly reduced when HCC cells were transfected with miR-200a or miR-183 mimics compared with control (Fig. 6C), while M1 and M3 increased significantly in HCC cells transfected with miR-200a or miR-183 mimics, and consistent results were observed in xenograft HCC model treated by sorafenib (Fig. 2C&E). Since UGT1A9 metabolism increased solubilization of sorafenib, decreased expression of MRCP, MRP-2, and P-gp transporters of hydrophilic sorafenib metabolites [12] might increase the cumulative dose in HCC cells. These data indicated that expression of UGT1A9 could be regulated by miR-200a and miR-183 and alter the pharmacokinetic distribution of sorafenib metabolites, which might subsequently affect the effectiveness of sorafenib in HCC patients.

In our study, we have found that miR-200a-3p/-183–5p could alter pharmacokinetic distribution of sorafenib metabolites. However, there is no notable difference in cell proliferation and apoptosis between miR-200a-3p/-183–5p and control cells when soraenib is administered in the culture system in in vitro. study (Supplementary Figs. 3B–3F). It is possible that miR-200a-3p/-183–5p might have a role on cell proliferation other than regulating UGT1A9 expression.

Although miR-200a-3p/-183–5p could regulate the expression of UGT1A9, the effect was not mutual (Supplementary Fig. 3A). miR-200a-3p/-183-5 have an effect on regulating sorafenib metabolites, however, miR-200a-3p/-183-5 overexpressing HCC cells didn't exhibit a higher inhibition rate in cell proliferation and apoptosis under the treatment of sorafenib *in vitro* (Supplementary Figs. 3B–3F). The expression of cancer stem cell biomarkers was slightly increased (Supplementary Fig. 3G) in HCC-LM3 miR-200a-3p cell lines. In another sorafenib treatment cohort (N = 52), data analysis indicated a negative correlation of UGT1A9 level and miR-200a-3p/-183–5p, however, miR-200a-3p/-183–5p was not relevant to overall survival or disease-free survival (Supplementary Figs. 4C–4F, Table 5-Table 9). Together, these data indicated the expression of UGT1A9 could be regulated by miR-200a and miR-183 and alter the pharmacokinetic distribution of sorafenib metabolites, which might subsequently affect the effectiveness of sorafenib in HCC patients.

In conclusion, this study identifies miRNA-200a and -183 as novel regulatory genes of UGT1A9 in HCC and demonstrates the clinical relevance of UGT1A9 in the prognosis of patients receiving sorafenib treatment. Since the 3′-UTR region is shared, it also provides a likely mechanism for posttranscriptional regulation of UGT1A family genes. These data shed light on the role of microRNAs as mediators of drug toxicity and efficacy.

Conflicts of interest

The authors have no conflicts of interest to declare.

Acknowledgments

The authors would like to thank Prof. Yusen Zhou from the Academy of Military Medical Science, Beijing, for the support provided, PMIR-report, and PMIR-control dual luciferase reporter plasmids.

Appendix A. Supplementary data

Supplementary data to this article can be found online at https://doi.org/10.1016/j.canlet.2019.03.030.

Funding

This study was supported by grants from the National Key R&D Program of China (2018YFC2000700), the Key Research Program (ZDRW-ZS-2017-1) of the Chinese Academy of Sciences, the National Nature Science Foundation (81630086, 81427805 and 81802878) and the Natural Science Foundation of Shandong Province (ZR2017LH008). This project is also sponsored by Shanghai Sailing Program (18YF1400200). The funders had no role in study design, data collection and analysis, decision to publish, or preparation of the manuscript.

References

[1] J. Ferlay, H.R. Shin, F. Bray, D. Forman, C. Mathers, D.M. Parkin, Estimates of worldwide burden of cancer in 2008: GLOBOCAN 2008, Int. J. Cancer 127 (2010) 2893–2917.
[2] D.M. Parkin, F. Bray, J. Ferlay, P. Pisani, Global cancer statistics, CA A Cancer J. Clin. 55 (2005) (2002) 74–108.
[3] S.F. Altekruse, K.A. McGlynn, M.E. Reichman, Hepatocellular carcinoma incidence, mortality, and survival trends in the United States from 1975 to 2005, J. Clin. Oncol. 27 (2009) 1485–1491.
[4] J.M. Llovet, J. Bruix, Molecular targeted therapies in hepatocellular carcinoma, Hepatology 48 (2008) 1312–1327.
[5] E.S. Knudsen, P. Gopal, A.G. Singal, The changing landscape of hepatocellular carcinoma: etiology, genetics, and therapy, Am. J. Pathol. 184 (2014) 574–583.
[6] G.M. Keating, A. Santoro, Sorafenib: a review of its use in advanced hepatocellular carcinoma, Drugs 69 (2009) 223–240.
[7] Z. Wang, J. Zhou, J. Fan, S.J. Qiu, Y. Yu, X.W. Huang, Z.Y. Tang, Effect of rapamycin alone and in combination with sorafenib in an orthotopic model of human hepatocellular carcinoma, Clin. Cancer Res. 14 (2008) 5124–5130.
[8] F. Gemignani, S. Landi, N. Szeszenia-Dabrowska, D. Zaridze, J. Lissowska, P. Rudnai, E. Fabianova, D. Mates, L. Foretova, V. Janout, V. Bencko, V. Gaborieau, L. Gioia-Patricola, I. Bellini, R. Barale, F. Canzian, J. Hall, P. Boffetta, R.J. Hung, P. Brennan, Development of lung cancer before the age of 50: the role of xenobiotic metabolizing genes, Carcinogenesis 28 (2007) 1287–1293.
[9] P. Vidjaya Letchoumy, K.V. Chandra Mohan, J.J. Stegeman, H.V. Gelboin, Y. Hara, S. Nagini, Pretreatment with black tea polyphenols modulates xenobiotic-metabolizing enzymes in an experimental oral carcinogenesis model, Oncol. Res. 17 (2008) 75–85.
[10] L.Q. Yang, S.J. Li, Y.F. Cao, X.B. Man, W.F. Yu, H.Y. Wang, M.C. Wu, Different alterations of cytochrome P450 3A4 isoform and its gene expression in livers of patients with chronic liver diseases, World J. Gastroenterol. 9 (2003) 359–363.
[11] R.H. Tukey, C.P. Strassburg, Human UDP-glucuronosyltransferases: metabolism, expression, and disease, Annu. Rev. Pharmacol. Toxicol. 40 (2000) 581–616.
[12] C. Asakawa, M. Ogawa, K. Kumata, M. Fujinaga, K. Kato, T. Yamasaki, J. Yui, K. Kawamura, A. Hatori, T. Fukumura, M.R. Zhang, [11C]sorafenib: radiosynthesis and preliminary PET study of brain uptake in P-gp/Bcrp knockout mice, Bioorg. Med. Chem. Lett 21 (2011) 2220–2223.
[13] D. Strumberg, H. Richly, R.A. Hilger, N. Schleucher, S. Korfee, M. Tewes, M. Faghih, E. Brendel, D. Voliotis, C.G. Haase, B. Schwartz, A. Awada, R. Voigtmann, M.E. Scheulen, S. Seeber, Phase I clinical and pharmacokinetic study of the Novel Raf kinase and vascular endothelial growth factor receptor inhibitor BAY 43-9006 in patients with advanced refractory solid tumors, J. Clin. Oncol. 23 (2005)

965–972.
[14] C. Lathia, J. Lettieri, F. Cihon, M. Gallentine, M. Radtke, P. Sundaresan, Lack of effect of ketoconazole-mediated CYP3A inhibition on sorafenib clinical pharmacokinetics, Cancer Chemother. Pharmacol. 57 (2006) 685–692.
[15] M.H. Court, S.X. Duan, L.L. von Moltke, D.J. Greenblatt, C.J. Patten, J.O. Miners, P.I. Mackenzie, Interindividual variability in acetaminophen glucuronidation by human liver microsomes: identification of relevant acetaminophen UDP-glucuronosyltransferase isoforms, J. Pharmacol. Exp. Ther. 299 (2001) 998–1006.
[16] O. Barbier, H. Girard, Y. Inoue, H. Duez, L. Villeneuve, A. Kamiya, J.C. Fruchart, C. Guillemette, F.J. Gonzalez, B. Staels, Hepatic expression of the UGT1A9 gene is governed by hepatocyte nuclear factor 4alpha, Mol. Pharmacol. 67 (2005) 241–249.
[17] D. Wiener, J.L. Fang, N. Dossett, P. Lazarus, Correlation between UDP-glucuronosyltransferase genotypes and 4-(methylnitrosamino)-1-(3-pyridyl)-1-butanone glucuronidation phenotype in human liver microsomes, Cancer Res. 64 (2004) 1190–1196.
[18] J.M. Hoskins, R.M. Goldberg, P. Qu, J.G. Ibrahim, H.L. McLeod, UGT1A1*28 genotype and irinotecan-induced neutropenia: dose matters, J. Natl. Cancer Inst. 99 (2007) 1290–1295.
[19] G. Chen, N.E. Giambrone Jr., D.F. Dluzen, J.E. Muscat, A. Berg, C.J. Gallagher, P. Lazarus, Glucuronidation genotypes and nicotine metabolic phenotypes: importance of functional UGT2B10 and UGT2B17 polymorphisms, Cancer Res. 70 (2010) 7543–7552.
[20] C.J. Gallagher, R.M. Balliet, D. Sun, G. Chen, P. Lazarus, Sex differences in UDP-glucuronosyltransferase 2B17 expression and activity, Drug Metab. Dispos. 38 (2010) 2204–2209.
[21] T. Izukawa, M. Nakajima, R. Fujiwara, H. Yamanaka, T. Fukami, M. Takamiya, Y. Aoki, S. Ikushiro, T. Sakaki, T. Yokoi, Quantitative analysis of UDP-glucuronosyltransferase (UGT) 1A and UGT2B expression levels in human livers, Drug Metab. Dispos. 37 (2009) 1759–1768.
[22] S. Oda, M. Nakajima, M. Hatakeyama, T. Fukami, T. Yokoi, Preparation of a specific monoclonal antibody against human UDP-glucuronosyltransferase (UGT) 1A9 and evaluation of UGT1A9 protein levels in human tissues, Drug Metab. Dispos. 40 (2012) 1620–1627.
[23] S. Ohtsuki, O. Schaefer, H. Kawakami, T. Inoue, S. Liehner, A. Saito, N. Ishiguro, W. Kishimoto, E. Ludwig-Schwellinger, T. Ebner, T. Terasaki, Simultaneous absolute protein quantification of transporters, cytochromes P450, and UDP-glucuronosyltransferases as a novel approach for the characterization of individual human liver: comparison with mRNA levels and activities, Drug Metab. Dispos. 40 (2012) 83–92.
[24] S. Ohno, S. Nakajin, Determination of mRNA expression of human UDP-glucuronosyltransferases and application for localization in various human tissues by real-time reverse transcriptase-polymerase chain reaction, Drug Metab. Dispos. 37 (2009) 32–40.
[25] Q. Ding, W. Xia, J.C. Liu, J.Y. Yang, D.F. Lee, J. Xia, G. Bartholomeusz, Y. Li, Y. Pan, Z. Li, R.C. Bargou, J. Qin, C.C. Lai, F.J. Tsai, C.H. Tsai, M.C. Hung, Erk associates with and primes GSK-3beta for its inactivation resulting in upregulation of beta-catenin, Mol. Cell 19 (2005) 159–170.
[26] Y. Xiong, J.H. Fang, J.P. Yun, J. Yang, Y. Zhang, W.H. Jia, S.M. Zhuang, Effects of microRNA-29 on apoptosis, tumorigenicity, and prognosis of hepatocellular carcinoma, Hepatology 51 (2010) 836–845.
[27] T. Yokoi, M. Nakajima, microRNAs as mediators of drug toxicity, Annu. Rev. Pharmacol. Toxicol. 53 (2013) 377–400.
[28] D.F. Dluzen, D. Sun, A.C. Salzberg, N. Jones, R.T. Bushey, G.P. Robertson, P. Lazarus, Regulation of UDP-glucuronosyltransferase 1A1 expression and activity by microRNA 491-3p, J. Pharmacol. Exp. Ther. 348 (2014) 465–477.
[29] L. Gong, M.M. Giacomini, C. Giacomini, M.L. Maitland, R.B. Altman, T.E. Klein, PharmGKB summary: sorafenib pathways, Pharmacogenetics Genom. 27 (2017) 240–246.
[30] N.P. van Erp, H. Gelderblom, H.J. Guchelaar, Clinical pharmacokinetics of tyrosine kinase inhibitors, Cancer Treat Rev. 35 (2009) 692–706.
[31] L. Ye, X. Yang, E. Guo, W. Chen, L. Lu, Y. Wang, X. Peng, T. Yan, F. Zhou, Z. Liu, Sorafenib metabolism is significantly altered in the liver tumor tissue of hepatocellular carcinoma patient, PLoS One 9 (2014) e96664.
[32] A.N. Edginton, E.I. Zimmerman, A. Vasilyeva, S.D. Baker, J.C. Panetta, Sorafenib metabolism, transport, and enterohepatic recycling: physiologically based modeling and simulation in mice, Cancer Chemother. Pharmacol. 77 (2016) 1039–1052.